



Characteristic and Source of Atmospheric PM₁₀- and PM_{2.5}-bound PAHs in a Typical Metallurgic City Near Yangtze River in China

Hong Zhang^{1,2} · Ruwei Wang¹ · Huaqin Xue¹ · Ruoyu Hu¹ · Guijian Liu¹

Received: 7 March 2017 / Accepted: 17 November 2017 / Published online: 25 November 2017
© Springer Science+Business Media, LLC, part of Springer Nature 2017

Abstract

The characteristics of atmospheric PM₁₀- and PM_{2.5}-bound polycyclic aromatic hydrocarbons (PAHs) were investigated in Tongling city, China. Results showed that the total concentrations of PM₁₀- and PM_{2.5}-bound PAHs exhibited distinct seasonal and spatial variability. The metallurgic sites showed the highest PAH concentrations, which is mainly attributed to the metallurgic activities (mainly copper ore smelting) and coal combustion as the smelting fuel. The rural area showed the lowest concentrations, but exhibited significant increase from summer to autumn. This seasonal fluctuation is mainly caused by the biomass burning at the sites in the harvest season. The diagnostic ratio indicated that the main PAHs sources were vehicle exhausts, coal combustion and biomass burning. The total BaP equivalent concentration (BAP-TEQ) was found to be maximum at DGS site in winter, whereas it was minimum at BGC site in summer. Risk assessment indicates that residential exposure to PAHs in the industrial area, especially in the winter season, may pose a greater inhalation cancer risk than people living in living area and rural area.

Keywords Polycyclic aromatic hydrocarbons · PM₁₀ and PM_{2.5} · Source identification · Diagnostic ratio · Tongling city

Polycyclic aromatic hydrocarbons (PAHs) are ubiquitous global contaminants and are potentially carcinogenic and mutagenic to human beings. Airborne PAHs can impact remote areas though long range transport due to their semi-volatile and persistent properties. In addition, they can deposit in the lungs and exert their carcinogenicity over long exposure periods. Some studies indicated that the carcinogenic 5- and 6-ring PAHs are often associated with the particle sizes below 2.0 μm (Ravindra et al. 2008). Therefore, it is necessary to investigate the characteristics and sources of ambient PM₁₀- and PM_{2.5}-bound PAHs. Substantial efforts have been dedicated to investigate the characteristics of PAHs in atmosphere. However, they mainly focused on the overall air quality in the megacities, there is lack of complex studies on atmospheric PAHs in the traditional metal mineral-based city.

Tongling city is located at the south bank of the lower middle reaches of Yangtze River (Fig. 1), which is a typical nonferrous industrial base for copper mining and smelting in China. As a result of the rapid development of industrial activities, traffic density and urbanization development, Tongling city has been suffering from serious air pollution of fine particulate matter in recent years. In this study, the characteristics and sources of atmospheric PM₁₀- and PM_{2.5}-PAHs from Tongling city were investigated. The aim of this study was to: (1) investigate the spatial and seasonal distribution of atmospheric PM₁₀- and PM_{2.5}-bound PAHs, (2) quantify the source contributions to PAHs, and (3) assess the carcinogenic risks of PAH exposure.

Materials and Methods

PM₁₀ and PM_{2.5} samples were collected at three sites representing different potential PAH sources, which include Dong Guashan (DGS) in industrial area, No.4 middle school (4MS) in central urban area, and Bei Gengcun (BGC) in rural areas (Fig. 1). 4MS (30°56'29", 117°49'4") is located in the city center with heavy traffic and busy commercial activities. DGS (30°55'53", 117°52'58") is located in the

✉ Guijian Liu
lgj@ustc.edu.cn

¹ CAS Key Laboratory of Crust-Mantle and the Environment, School of Earth and Space Sciences, University of Science and Technology of China, Hefei, Anhui, China

² Anhui Environment Science Institute, Hefei 230021, Anhui, China

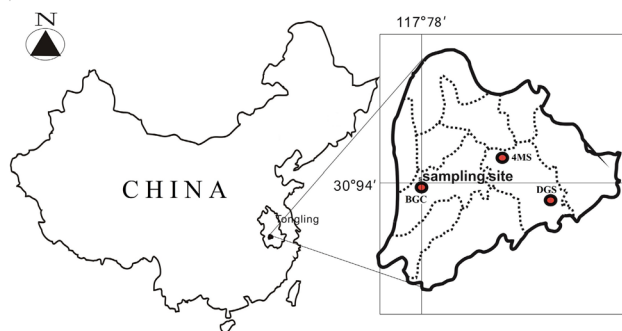


Fig. 1 Map of the studied area with sampling sites

mining zones surrounded by concentric mining activities. BGC (30°55'53", 117°43'13") is located in a small town surrounded by farmlands in the surrounding, and 940 m from the Yangtze River.

Sampling campaign was conducted continuously in the period of August, September, October, November, December and January from 2014 to 2015. PM₁₀ and PM_{2.5} particle fractions were collected using a medium-volume air sampler (TH150D, manufactured by Wuhan Tianhong Ltd, China). PM₁₀ and PM_{2.5} samples were collected on quartz filters (Whatman Company, UK with 90 diameter) which were baked at 550°C for 4 h before sampling. Each sample was collected for 20 h with a flow rate of 100 L/min. Samples were collected under both haze and non-haze conditions in July–Aug, Oct–Nov and Jan–Feb respectively in 2014.

Before sample-extraction, a mixture of surrogate standards 2-fluoro-1,1-biphenyl, p-terphenyl-d₁₄ and dibenzo[a,h]anthracene-d₁₄ (Cambridge Isotope Laboratories) were added to the filters. Each sample was extracted using an accelerated solvent extraction (ASE) apparatus with 15 mL mixture solution of dichloromethane (DCM) and acetone for 10 min. Then the extracts were processed by concentration, solvent-exchange and elution. Determination of PAHs was performed using an Agilent gas chromatograph mass spectrometer (GC-MS, GC 6890 and MSD 5973N) equipped with a 30 m × 0.25 mm i.d. HP-5 column with film thickness of 0.25 μm. Sixteen US EPA priority PAH species were detected including naphthalene (Naph), acenaphthylene (Acy), acenaphthene (Acen), fluorene (Flu), phenanthrene (Phen), anthracene (Anth), Fluoranthene (Fluo), Pyrene (Pyr), benz[a]anthracene (BaA), chrysene (Chr), benzo[b]fluoranthene (BbF), benzo[k]fluoranthene (BkF), benzo[a]pyrene (BaP), dibenzo[a,h]anthracene (DahA), indeno[1,2,3-cd]pyrene (IP), benzo[ghi]perylene (BghiP).

Quality assurance was provided by analysing 1 of 4 samples in duplicate (samples split in the laboratory), recovery of surrogate compounds and analytical blanks. The average recovery rates were 87.3%, 82.5% and 81.8% for anthracene-d₁₀, pyrene-d₁₀ and 1-nitro-pyrene-d₉, respectively.

Analytical blanks were used as a control at each step of the analyses. Detection limits (DLs) were set to the lowest concentration of the calibration standard, and three times the signal-to-noise found in the procedural blanks.

Result and Discussion

As shown in Tables 1 and 2, PM₁₀ and PM_{2.5} concentrations in the summer show the lowest pollution level compared with those in autumn and winter (Tables 1, 2), which may be resulted from the higher precipitation resulting from the summer monsoon (Wang et al. 2015). Moreover, the total concentrations of PM-bound PAHs (Σ₁₆PAHs) at DGS site are significantly higher than those at 4MS site and BGC site. This is not unexpected since that the sampling site of DGS was surrounded by many coal mining and smelting factories, where coal combustion may increase the atmospheric PAH concentrations. Moreover, the transport of coal and ores may also increase the atmospheric PAH levels due to the resuspended dusts and vehicle exhausts.

Various groups have investigated the characteristics of atmospheric PAHs in different cities around the world. Their concentrations varied widely from ca. 0.05 to ca. 449 ng/m³, depending on the locations where the samples were collected. For example, PAH concentrations in our work are much lower than those reported in Beijing (258.2 ± 208.8 ng/m³) (Guo et al. 2016), whereas they are significantly higher than those reported in Guangzhou (0.29–56.9 ng/m³) (Yu et al. 2016), Nanjing (3.87–15.6 ng/m³) (Li et al. 2016) and Sanya (0.8–220 ng/m³) and Shanghai (6.41–7.48 ng/m³) (Wang et al. 2015).

On the other hand, the highest PAH concentrations in winter were at DGS site (167.51 ± 10.94 and 76.38 ± 2.74 ng/m³ in PM₁₀ and PM_{2.5} fractions, respectively), followed by 4MS site (113.42 ± 5.91 and 65.67 ± 5.08 ng/m³ in PM₁₀ and PM_{2.5} fractions, respectively) and BGC site (82.5 ± 9.17 and 55.36 ± 3.01 ng/m³ in PM₁₀ and PM_{2.5} fractions, respectively). In contrast, PAH concentrations showed the lowest level in summer. Moreover, PAH concentrations in PM₁₀ and PM_{2.5} fractions in autumn showed significant increase at BGC site compared with those in summer. The seasonal variation trend of atmospheric PAH concentrations is consistent with some previous studies (Chen et al. 2011; Callén et al. 2014), which suggested that the increased ambient temperature and intense sunlight in summer may cause PAH degradation in a larger extent, thus resulting in lower atmospheric PAH concentration. In addition, the decreased ambient temperature, slower photolysis and radical degradation reaction of PAHs in winter may increase the atmospheric PAH concentrations.

Moreover, the normalized PAH concentrations (NC) values across three sites and seasons, which is calculated based

Table 1 PAH concentrations in PM₁₀ fractions (mean ± SD, ng/m³)

PAHs and PMs	DGS			4MS			BGC		
	Summer (n=4)	Autumn (n=5)	Winter (n=3)	Summer (n=4)	Autumn (n=5)	Winter (n=3)	Summer (n=4)	Autumn (n=4)	Winter (n=3)
Nap	1.23±0.26	1.15±0.27	1.82±0.18	0.87±0.34	0.92±0.26	0.66±0.26	0.61±0.15	0.95±0.49	0.58±0.1
Acy	2.25±0.28	3.63±0.48	4.87±0.57	1.91±0.33	2.18±0.36	2.43±0.34	1.02±0.2	2.85±0.42	2.81±0.45
Acen	2.87±0.51	4.36±0.6	6.75±0.64	1.75±0.5	3.37±0.9	4.03±0.37	1.77±0.21	3.74±0.51	4.18±0.92
Flu	3.05±0.34	5.86±0.38	8.64±0.29	2.13±0.33	4.82±1.23	5.39±0.41	3.08±0.49	4.41±1.12	5.36±1.18
Phen	3.16±0.88	5.97±0.7	9.82±0.49	3.86±0.61	4.25±0.66	5.41±1.0	4.04±0.54	3.48±0.88	5.85±1.07
Anth	3.49±0.87	7.37±0.31	10.05±0.71	4.05±0.39	4.92±0.94	6.47±0.42	3.92±0.42	4.22±1.39	6.54±0.68
Fluo	8.87±1.11	14.38±0.55	12.69±1.67	4.61±0.4	8.68±1.53	7.66±0.51	3.86±0.38	7.28±1.01	8.13±1.17
Pyr	9.21±0.37	5.87±0.42	5.95±1.53	7.92±2.12	5.56±0.5	5.44±0.41	4.80±1.34	5.22±1.22	5.70±0.85
BaA	8.25±0.82	9.36±0.42	13.37±2.05	5.21±0.43	7.81±0.50	9.26±0.72	3.95±0.46	5.94±1.1	4.92±0.3
Chr	7.56±0.49	10.14±1.0	15.36±1.22	3.36±0.57	7.02±1.0	10.05±0.72	4.11±0.59	6.11±1.18	6.04±0.48
BbF	5.52±0.49	12.37±1.14	16.25±1.75	4.86±0.35	6.63±0.63	11.24±0.69	5.25±0.7	7.16±1.81	6.37±0.19
BkF	8.61±0.35	10.67±0.32	12.28±0.98	4.39±0.6	7.86±1.7	6.72±0.22	3.57±0.78	7.54±1.12	6.55±0.79
BaP	8.18±0.72	10.96±0.95	14.36±2.23	3.97±0.75	7.02±0.63	9.79±0.5	4.82±0.72	7.05±0.68	5.93±0.54
DahA	6.75±0.7	10.27±0.3	15.96±2.4	5.66±0.62	6.25±0.56	11.03±2.38	3.41±0.83	5.03±0.89	4.91±0.52
IP	7.46±0.48	9.28±0.86	12.96±0.52	4.65±0.73	8.25±1.18	10.78±0.65	4.77±0.52	6.36±0.75	5.37±0.69
BghiP	8.76±0.8	5.23±0.59	6.38±0.89	6.27±0.73	6.22±1.16	7.06±0.81	6.45±0.58	3.28±0.46	3.26±0.61
PM ₁₀ (µg/m ³)	91.75±4.1	107.91±3.26	147.47±3.81	86.11±3.4	95.24±4.06	133.37±8.1	66.55±4.53	83.81±3.49	118.01±4.75
NC ^a (mg/g)	1.04±0.09	1.18±0.05	1.14±0.12	0.76±0.11	0.96±0.07	0.85±0.04	0.90±0.12	0.96±0.08	0.70±0.08
Total PAHs	95.22±4.48	126.87±2.32	167.51±10.94	65.47±7.18	91.76±7.09	113.42±5.91	59.43±3.02	80.62±7.83	82.50±9.17

^aNC normalized PAH concentration (mg/g)

Table 2 PAH concentrations in PM_{2.5} fractions (mean ± SD, ng/m³)

PAHs species	DGS			4MS			BGC		
	Summer (n=4)	Autumn (n=5)	Winter (n=3)	Summer (n=4)	Autumn (n=5)	Winter (n=3)	Summer (n=4)	Autumn (n=4)	Winter (n=3)
Nap	0.76±0.13	0.81±0.31	0.82±0.24	0.73±0.24	0.69±0.30	0.88±0.27	0.69±0.21	0.72±0.30	0.77±0.24
Acy	0.91±0.18	0.86±0.32	0.97±0.24	0.79±0.28	1.05±0.32	1.29±0.20	0.76±0.27	1.12±0.29	1.28±0.22
Acen	0.81±0.28	1.57±0.56	1.02±0.27	0.78±0.27	1.31±0.29	1.73±0.63	0.76±0.19	1.13±0.27	1.65±0.22
Flu	0.83±0.32	1.22±0.37	0.93±0.18	0.82±0.27	1.79±0.53	1.98±0.44	0.85±0.37	1.37±0.18	1.47±0.27
Phen	1.52±0.29	2.55±0.56	3.88±0.56	1.42±0.32	1.95±0.49	3.11±0.47	1.35±0.55	1.75±0.44	2.23±0.29
Anth	1.62±0.55	2.73±0.59	5.94±0.44	1.47±0.52	2.51±0.59	3.07±0.30	2.31±0.81	2.65±0.35	3.77±0.48
Fluo	4.20±0.51	6.26±0.92	5.91±0.37	2.94±0.72	5.96±1.02	5.83±0.38	1.93±0.42	4.82±0.81	5.01±0.58
Pyr	4.93±0.45	4.04±0.26	3.93±0.30	4.52±0.28	4.56±0.61	4.51±0.62	2.68±0.51	2.97±0.52	3.87±1.17
BaA	3.26±0.45	6.87±0.54	6.25±0.59	3.74±0.40	4.51±0.41	6.26±0.77	2.72±0.23	4.74±0.51	4.87±0.85
Chr	3.75±0.34	6.17±0.66	7.12±0.62	2.47±0.40	5.73±0.99	5.37±0.72	2.37±0.59	4.28±1.10	4.39±0.85
BbF	4.17±0.55	6.24±0.52	7.26±0.48	3.74±0.78	4.28±0.50	4.98±0.38	1.62±0.43	3.96±0.35	5.41±0.79
BkF	5.02±0.52	5.96±0.46	6.97±0.47	3.96±0.43	3.94±1.19	5.46±0.71	1.98±0.62	4.75±1.20	3.92±0.46
BaP	4.28±0.62	5.27±0.66	6.39±0.73	4.02±0.30	4.68±0.45	5.73±0.36	2.17±0.55	3.87±0.42	4.87±1.01
DahA	3.11±0.58	4.52±0.61	5.92±0.41	3.24±0.31	4.97±0.51	4.04±0.68	1.89±0.39	4.87±0.36	4.51±0.58
IP	4.68±0.45	6.26±0.85	7.19±0.63	3.52±0.45	5.26±1.15	6.81±0.80	3.01±0.51	4.71±0.39	4.35±0.62
BghiP	6.73±0.85	5.09±0.64	5.88±0.46	5.45±0.56	4.04±0.96	4.62±0.48	4.16±0.61	3.62±0.36	2.99±0.37
PM _{2.5} (µg/m ³)	62.11±4.05	67.17±5.06	77.89±2.82	56.18±1.81	55.96±0.88	69.16±4.06	47.47±4.96	54.49±3.44	67.54±3.68
PM _{2.5} /PM ₁₀	0.65±0.02	0.56±0.02	0.53±0.03	0.65±0.02	0.59±0.02	0.52±0.02	0.71±0.04	0.65±0.02	0.58±0.02
NC ^a (mg/g)	0.86±0.08	1.09±0.07	0.98±0.07	0.78±0.05	1.02±0.07	0.95±0.06	0.67±0.15	0.95±0.03	0.82±0.06
Total PAHs	50.58±1.62	66.42±2.36	76.38±2.74	43.61±2.05	57.23±4.39	65.67±5.08	31.25±3.49	51.33±4.55	55.36±3.01

^aNC normalized PAH concentration (mg/g)

on the division of PAH concentration by PM mass concentration, are shown in Tables 1 and 2, respectively. It can be seen that the NC values for both PM_{10} and $PM_{2.5}$ at BGC site are lower than those at DGS and 4MS sites, in contrast, the NC values at DGS are the highest across both three seasons. This indicates that the atmospheric PAHs at urban and rural area are less influenced by the local emissions when compared with the industrial site. In addition, the NC values for both the PM_{10} and $PM_{2.5}$ in summer are lower than those in autumn and winter, especially for the NC value derived from $PM_{2.5}$ fraction in summer, suggesting that atmospheric PAHs in summer are more influenced by the evaporation and/or atmospheric transportation rather than the local emission.

Previous studies have indicated that the abundance ratios (AR) of $PM_{2.5}/PM_{10}$ can be used to differentiate their sources (Zhou et al. 2016). Higher ratios (>0.6) indicate

the greater contributions by secondary particulate formation from inorganic matter and partial organic matter, whereas lower ratios indicate the primary sources for mineral dusts from re-suspended soil and road dust. Table 2 shows that the AR ratios of $PM_{2.5}/PM_{10}$ at remote site (BGC) are generally higher than those at industrial site (DGS) and city center (4MS) influenced by anthropogenic local source. In addition, the AR ratios of $PM_{2.5}/PM_{10}$ are higher in summer than that in winter and autumn, suggesting the enhanced production and accumulation of secondary $PM_{2.5}$ in the summer.

The PAH profiles in function of the different number of rings are illustrated in Fig. 2. The 4- to 6-ring PAHs are predominant in both PM_{10} - and $PM_{2.5}$ -phases, accounting for 69.2%–83.1% and 78.5%–87.2% of total PAHs, respectively (Fig. 2a, b). In addition, PAH profiles varied at different sampling sites, suggesting their different PAH sources. For

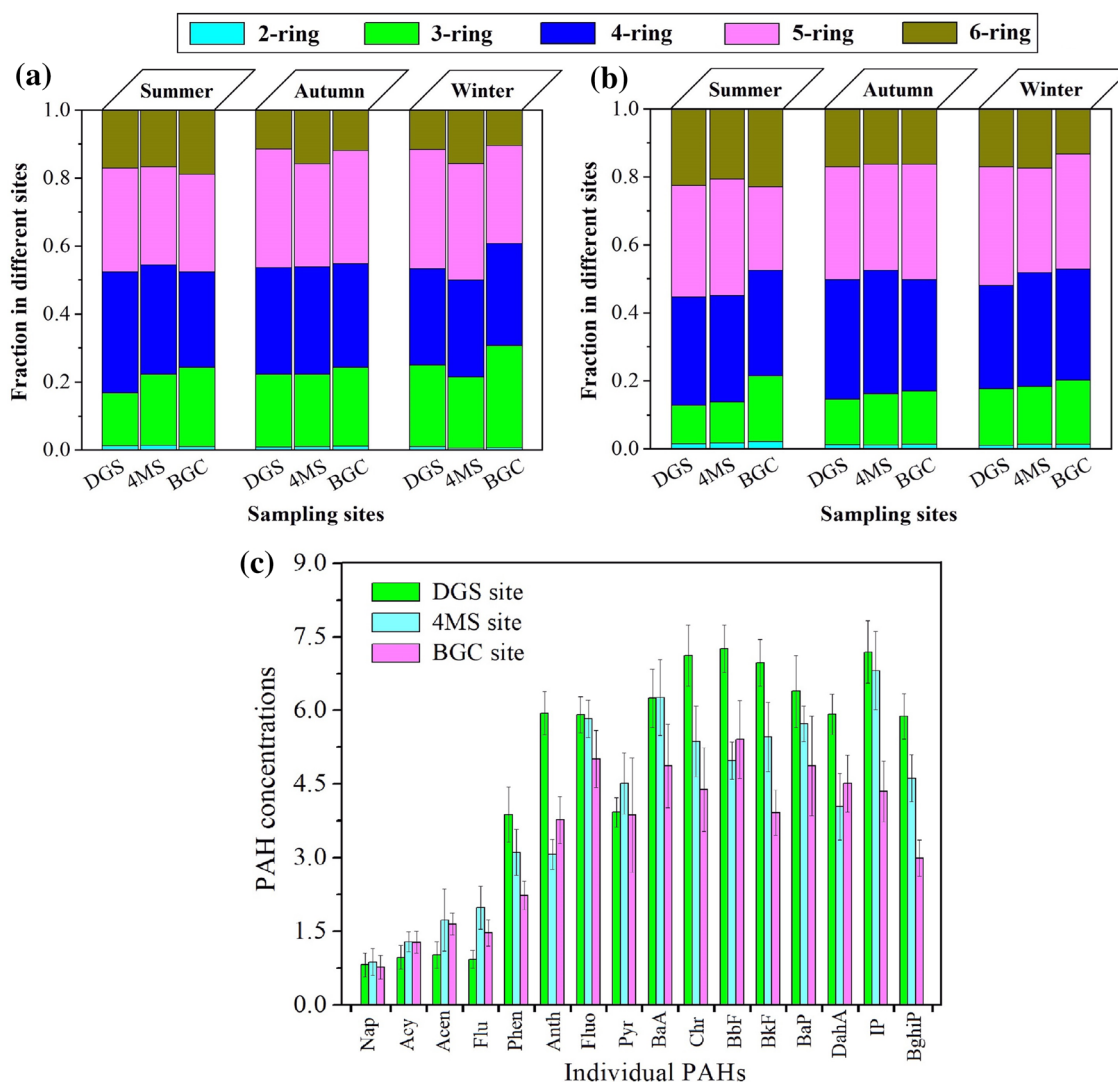


Fig. 2 PAH concentration fractions of different aromatic rings and individual PAH concentrations. **a** PM_{10} ; **b** $PM_{2.5}$; **c** $PM_{2.5}$ -bound PAHs in winter

example, the fractions of 2- and 3-ring PAHs increased as BGC > 4MS > DGC, suggesting that the atmospheric PAHs levels at rural site were mainly affected by PAH evaporation, whereas those at industrial site were mainly affected by the local PAH emissions.

Nevertheless, correlations between the ring size distributions need to be used with caution because PAH profiles in the sampling locations may be different from those in the source sites (Wu et al. 2005), since the occurrence of chemical reaction with other atmospheric pollutants (e.g. NO_x and O₃) and/or degradation during the sampling process can modify the apparent atmospheric PAH levels (Robinson et al. 2006). More detailed analysis of the distribution of the individual PAHs in winter between different sites is given in Fig. 2c. It can be seen that the concentrations of medium (MMW) and high molecular weight (HMW) PAHs (from Fluor to BghiP) at DGS site are higher than those at 4MS and BGC sites, which is opposite to the low molecular weight (LMW) PAHs (from NaP to Phen). This further supports that the atmospheric PAHs has distinct sources at DGS site from those at 4MS and BGC sites. Moreover, in contrast to the MMW and HMW PAHs, the relative concentrations of LMW PAHs (i.e., NaP, Acy and Acen) at BGC site are higher than those at DGS and 4MS sites, especially for Anth which shows significant higher concentration than that at 4MS site (Fig. 2c), supporting the assumption that atmospheric PAHs at rural site are mainly derived from the PAH evaporation.

PAH molecular diagnostic ratios, such as Anth/(Anth + Phen), Flu/(Flu + Pyr), BaA/(BaA + Chr), IP/(IP + BghiP) and BaP/BghiP, have been extensively studied and successfully used as qualitative tools to characterize and identify possible emission sources (Yunker et al. 2002; Ding et al. 2007; Ahad et al. 2015). This methodology is based on the assumption that paired isomers are diluted to a similar

extent during transport, and the ratios remain constant from the sources to the receptors (Katsoyiannis et al. 2011). In this work, the combination of Flu/(Flu + Pyr) versus IP/(IP + BghiP) for PM₁₀-bound PAHs were further employed to apportion PAH sources (Fig. 3a, b). Yunker et al. (2002) proposed that the scatter plots of Flu/(Flu + Pyr) versus IP/(BghiP + IP) with boundary values are (< 0.2, < 0.4) for petroleum, (0.2–0.5, 0.4–0.5) for petroleum combustion and (> 0.5, > 0.5) for grass/wood/coal combustion. The ratios of Flu/(Flu + Pyr) at both sampling sites are highly consistent in summer, which varied between 0.37 and 0.49 for PM₁₀-bound PAHs as well as between 0.39 and 0.46 for PM_{2.5}-bound PAHs, respectively (Fig. 3a, b). This indicates that vehicular traffic emission has greater contribution to atmospheric PAHs in summer for both sampling sites, which is supported by the ratio values of IP/(IP + BghiP) ranging from 0.42 to 0.46 for PM₁₀-bound PAHs and 0.39 to 0.42 for PM_{2.5}-bound PAHs, respectively (Fig. 3a, b). In contrast, the ratio values of Flu/(Flu + Pyr) and IP/(IP + BghiP) at 4MS and DGS sites in autumn and winter were significantly larger than 0.5 (Fig. 3a, b), indicating that grass/wood/coal combustion were the main source of PAHs at central urban and industrial sites. The observed diagnostic ratios indicate that biomass burning in rural areas has less contribution to atmospheric PAHs in summer, whereas it has significant contribution in autumn and winter. Vehicular traffic emission greatly contribute to the atmospheric PAHs in summer in city center and industrial areas, whereas coal combustion dominated the atmospheric PAH pollution in winter in these areas.

It must be noted that diagnostic ratios that incorporate LMW species should be used with caution because they are largely present in vapour phase v.s. HMW species which are largely in particle phase. In addition, LMW species are greater volatilized to vapour phase in summer due to their

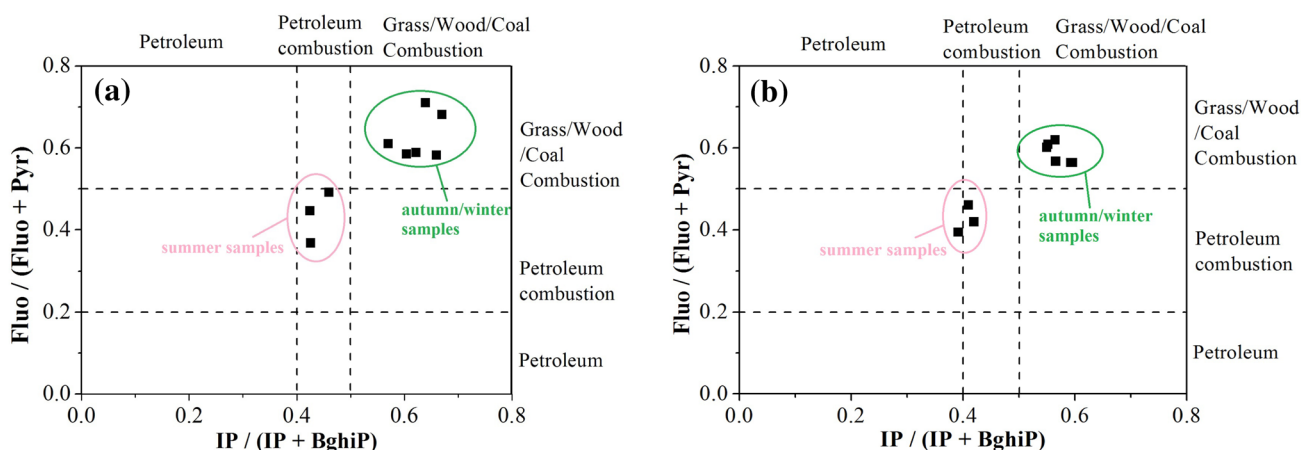


Fig. 3 PAH cross plots for the ratios of IP/(IP+BghiP) v.s. Flu/(Flu+Pyr) in **a** PM₁₀ fraction; **b** PM_{2.5} fraction in Tongling city of different seasons

higher vapour pressure, which also limit the accuracy of diagnostic method for source apportionment (Galarneau 2008). Moreover, some reference values exhibited inconsistencies for PAHs emitted from different sources. For example, the values of IP/(IP + BghiP) reported by Ravindra et al. (2006) for diesel exhaust (0.37), wood (0.62) and coal combustion (0.56) fell in the range of those for diesel exhaust (0.35–0.7) reported by Rogge et al. (1993).

The application of BAP-equivalent toxicity (BAP-TEQ) calculating by multiplying concentrations by appropriate toxicity equivalency factors (TEFs), as illustrated in Eq. (1), is frequently used to estimate the carcinogenic potency of atmospheric PAHs.

$$\text{BAP-TEQ} = \sum_i C_i \times \text{TEF}_i \quad (1)$$

where C_i is the concentration of targeted individual PAHs, TEF_i is the corresponding toxic equivalency factor, which were proposed by Nisbet and LaGoy (1992) based on the knowledge of PAH carcinogenic effects. It should be noted that this method of risk assessment might underestimate risk due to the fact that not all PAHs, but only limited compounds, are considered (Jung et al. 2010). The calculated BAP-TEQ values showed that PAH pollution levels in winter are higher than those in summer and autumn. In addition, the BAP-TEQ values was found to be maximum at DGS site (99.9 ± 14.2 and 38.9 ± 3.2 ng/m³ in PM₁₀ and PM_{2.5}, respectively) in winter and minimum at BGC site in summer (23.7 ± 3.8 and 12.6 ± 2.0 ng/m³ in PM₁₀ and PM_{2.5}, respectively). Apparently, people living in the industrial area may pose a greater inhalation cancer risk than people living in living area and rural area.

In conclusion, the concentrations of PAHs in PM₁₀ and PM_{2.5} were measured in central urban, industrial and rural sites in different seasons of Tongling city. The PAHs concentrations varied from 59.43 to 167.51 ng/m³ and 31.25 to 76.38 ng/m³ in PM₁₀ and PM_{2.5}, respectively. Distinct seasonal and spatial variability has been observed in the PM₁₀- and PM_{2.5}-bound PAHs, which is attributed to difference in emission sources. PAHs in industrial area showed significantly higher levels than those in central urban area and rural area. Moreover, PAHs in autumn exhibited sharp increase in the rural area compared to the summer. PAHs released from the common practice of straw burning in northern Anhui province might transfer to Tongling city along with the general atmospheric circulation. Diagnostic ratios confirm that vehicle exhaust emissions, coal combustion, biomass burning were the predominant sources of atmospheric PAHs in Tongling, albeit their contribution proportions vary in different functional areas and seasons.

Acknowledgements The work was supported by National Key R&D Program of China (2016YFC0201600), National Natural Science

Foundation of China (41403076, 41773099), Natural Science Foundation of Anhui Province (1604f0804001). We thank the editor Erin Bennett and anonymous reviewers for their thoughtful comments.

References

- Ahad JME, Hautzy JJ, Cumming BF, Das B, Laird KR, Sanei H (2015) Sources of polycyclic aromatic hydrocarbons (PAHs) to north-western Saskatchewan lakes east of the Athabasca oil sands. *Org Geochem* 80:35–45
- Callén MS, Iturmendi A, López JM, Mastral AM (2014) Source apportionment of the carcinogenic potential of polycyclic aromatic hydrocarbons (PAH) associated to airborne PM₁₀ by a PMF model. *Environ Sci Pollut Res* 21:2064–2076
- Chen YJ, Feng YL, Xiong SC, Liu DY, Wang G (2011) Polycyclic aromatic hydrocarbons in the atmosphere of Shanghai, China. *Environ Monit Assess* 172:235–247
- Ding X, Wang XM, Xie ZQ, Xiang CH, Mai BX, Sun LG et al (2007) Atmospheric polycyclic aromatic hydrocarbons observed over the North Pacific Ocean and the Arctic area: spatial distribution and source identification. *Atmos Environ* 41:2061–2072
- Galarneau E (2008) Source specificity and atmospheric processing of airborne PAHs: implications for source apportionment. *Atmos Environ* 42:8139–8149
- Guo XY, Li G, Gao Y, Tang L, Briki M, Ding HJ, Ji HB (2016) Sources of organic matter (PAHs and n-alkanes) in PM_{2.5} of Beijing in haze weather analyzed by combining the C–N isotopic and PCA–MLR analyses. *Environ Sci* 18:314–322
- Jung KH, Yan BZ, Chillrud SN, Perera FP, Whyatt R, Camann D, Kinney PL, Miller RL (2010) Assessment of benzo(a)pyrene-equivalent carcinogenicity and mutagenicity of residential indoor versus outdoor polycyclic aromatic hydrocarbons exposing young children in New York city. *Int J Environ Res Public Health* 7:1889–1990
- Katsoyiannis A, Sweetman A, Jones K (2011) PAH molecular diagnostic ratios applied to atmospheric sources: a critical evaluation using two decades of source inventory and air concentration data from the U.K. *Environ Sci Technol* 45:8897–8906
- Li XX, Kong SF, Yin Y, Li L, Yuan L, Li Q, Xiao H, Chen K (2016) Polycyclic aromatic hydrocarbons (PAHs) in atmospheric PM_{2.5} around 2013 Asian Youth Games period in Nanjing. *Atmos Res* 174–175:85–96
- Nisbet I, LaGoy P (1992) Toxic equivalency factors (TEFs) for polycyclic aromatic hydrocarbons (PAHs). *Regul Toxicol Pharmacol* 16:290–300
- Ravindra K, Bencs L, Wauters E, Hoog JD, Deutsch F, Roekens E et al (2006) Seasonal and site specific variation in vapor and aerosol phase PAHs over Flanders (Belgium) and their relation with anthropogenic activities. *Atmos Environ* 40:771–785
- Ravindra K, Sokhia R, Van Grieken R (2008) Atmospheric polycyclic aromatic hydrocarbons: source attribution, emission factors and regulation: a review. *Atmos Environ* 42:2895–2921
- Robinson AL, Subramanian R, Donahue NM, Rogge WF (2006) Source apportionment of molecular markers and organic Aerosol 1. Polycyclic aromatic hydrocarbons and methodology for data visualization. *Environ Sci Technol* 40:7803–7810
- Rogge WF, Hidemann LM, Mazurek MA, Cass GR, Simoneit BRT (1993) Sources of fine organic aerosol: 2. Noncatalyst and catalyst-equipped automobiles and heavy-duty diesel trucks. *Environ Sci Technol* 27:636–651
- Wang JZ, Ho SSH, Cao JJ, Huang RJ, Zhou JM, Zhao YZ, Xu HM, Liu SX, Wang GH, Shen ZX, Han YM (2015) Characteristics and major sources of carbonaceous aerosols in PM_{2.5} from Sanya, China. *Sci Total Environ* 530–531:110–119

- Wu SP, Tao S, Zhang ZH, Lan T, Zuo Q (2005) Distribution of particle-phase hydrocarbons, PAHs and OCPs in Tianjin, China. *Atmos Environ* 39:7420–7432
- Yu QQ, Gao B, Li GH, Zhang YL, He QF, Deng W, Huang ZH, Ding X, Hu QH, Huang ZZ, Wang YJ, Bi XH, Wang XM (2016) Attributing risk burden of PM_{2.5}-bound polycyclic aromatic hydrocarbons to major emission sources: case study in Guangzhou, south China. *Atmos Environ* 142:313–323
- Yunker MB, Macdonal RW, Vingarzan R, Mitchell RH, Goyette D, Sylvestre S (2002) PAHs in the Fraser river basin: a critical appraisal of PAH ratios as indicators of PAH source and composition. *Org Geochem* 33:489–515
- Zhou XH, Cao ZY, Ma YJ, Wang LP, Wu RD, Wang WX (2016) Concentrations, correlations and chemical species of PM_{2.5}/PM₁₀ based on published data in China: potential implications for the revised particulate standard. *Chemosphere* 144:518–526